Conformational control of *ortho*-phenylenes by terminal amides

Govinda Prasad Devkota[1], William P. Carson[1], and C. Scott Hartley[1,*]

[1]Department of Chemistry & Biochemistry, Miami University, Oxford, Ohio 45056, United States

[*]scott.hartley@miamioh.edu

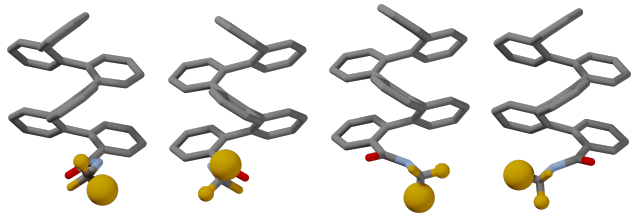

Abstract

Control over the folding of oligomers, be it broad induction of a preferred helical handedness or subtle changes in the orientations of individual functional groups, is important for applications ranging from molecular recognition to long-range conformational communication. Here, we report a series of *ortho*-phenylene hexamers functionalized with achiral and chiral amides at their termini. NMR spectroscopy, taking advantage of ^{19}F labeling, allows multiple conformers to be detected for each compound. In combination with CD spectroscopy and DFT calculations, specific geometries corresponding to each conformer have been identified and quantified. General conclusions about the effect of sterics and the amide linker on conformational behavior have been drawn, revealing

some similarities and key differences with previously reported imines. A model for twist sense control has been developed that is supported by computational models.

1 Introduction

The complex, stereoselective folding of biomacromolecules is necessary for the operation of many biochemical systems. "Foldamers", synthetic oligomers that fold into well-defined structures, have consequently been developed that mimic the hierarchical structure of biomacromolecules.[1–3] A variety of helical aromatic foldamers have been reported that show unique structures, properties, and dynamic behavior.[4–6] Basic aromatic repeat units are achiral, and so their folding will not inherently show any preference toward a specific handedness. However, stereochemical control of their folding is of great importance for their potential practical applications in asymmetric catalysis[7] and molecular recognition.[8,9] This can be achieved for aromatic foldamers by attaching chiral groups either as side chains[10–14] or to the termini.[15–26]

The *ortho*-phenylenes are simple aromatic foldamers that fold into helical geometries in solution driven by arene–arene stacking interactions.[27,28] *o*-Phenylenes offer an attractive combination of properties that makes them well-suited to the study of folding in solution: their folding is dynamic, tunable, and described by straightforward models, and there is a predictable relationship of their NMR properties to their geometries. To control the handedness of *o*-phenylene folding, we have previously studied the behavior of *o*-phenylenes functionalized with chiral imines at their termini, including the compounds in Chart 1a.[29] A combination of computational chemistry, NMR spectroscopy, and CD spectroscopy yielded two key conclusions. First, greater chiral induction was observed by attaching chiral groups ortho to the backbone (as in Chart 1a), where they are closer to the helix and can interact with it more strongly. Second, chiral induction in this system is highly dependent on broader conformational behavior. There is a strong coupling between the ability of substituents to

induce a preferred twist sense and their orientational preferences with respect to the helix. For example, simple chiral groups are "ambidextrous", inducing a left-handed helix in one orientation but right handed in another.

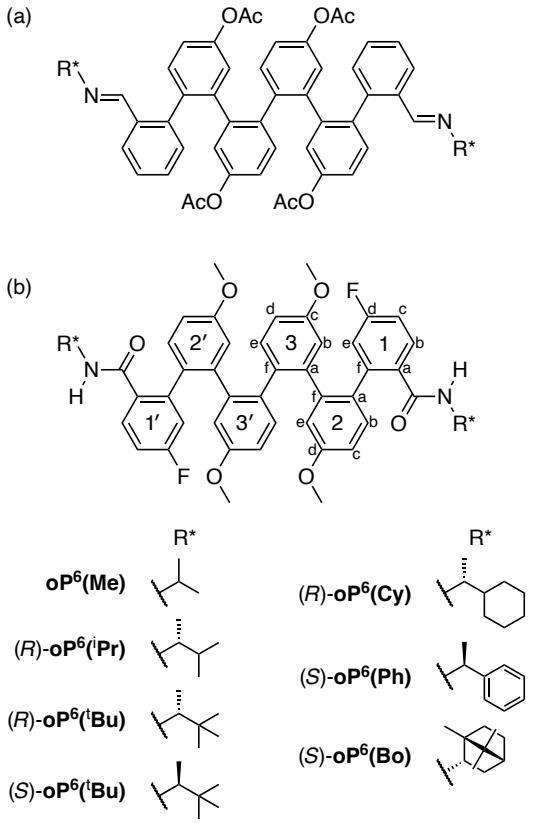

Chart 1: (a) Previously studied imine-functionalized *o*-phenylenes. (b) Amide-functionalized *o*-phenylene hexamers studied here, with labels used for NMR analysis.

The imines in Chart 1a showed that, beyond simply inducing a preferred twist sense in the oligomer, there can be a close connection between fine-grained conformational behavior and chiral induction in *o*-phenylene systems. Understanding this connection could be of interest as a way to communicate chiral information over distances through the foldamer,[30,31] or as a means to amplify small-scale chemical changes as large-amplitude changes in folding.[32] The dynamic nature of imines,[33] however, complicates such studies. Moreover, the generality of this behavior beyond imines is unknown.

Here, we report the behavior of the series of amide-functionalized *o*-phenylenes in Chart 1b. We focus on amides because of their stability, their structural similarity to the previously

reported imines, their synthetic convenience, and the ready availability of enantiomerically pure amine starting materials. Attachment at the ortho position allows the amides to reorient with respect to the *o*-phenylene helix, potentially giving rich conformational behavior. Oligomer geometries were studied using NMR spectroscopy, CD spectroscopy, and computational methods. We obtain a detailed picture of the effect of amide structure on *o*-phenylene conformation, determining the effects both on local geometry and the overall twist sense. From this we obtain structure–property relationships relating amide structure to folding and a model for twist sense induction.[34]

2 Results

2.1 Design and synthesis

We focused on *o*-phenylene hexamers because they are long enough that the oligomer is in slow conformational exchange on the NMR time scale[35] but short enough that the NMR spectra should be tractable even for the expected mixtures of conformers. The fluoro groups were included to help with the NMR analysis, as we have previously shown that ^{19}F NMR chemical shifts are sensitive to *o*-phenylene backbone conformations and can be used to detect and quantify the folding populations of different conformers, complementing ^{1}H and ^{13}C based spectra.[36] The methoxy groups along the backbone were included to ensure solubility; they were not exchanged late in the synthesis for the acetoxy groups used for the imines (Chart 1a) because it was not found to be necessary to improve folding. The seven different oligomers with different amide groups in Chart 1b were synthesized as described in the Supporting Information (Scheme S3). Unfortunately, attempts to grow crystals of the oligomers suitable for crystallography were unsuccessful.

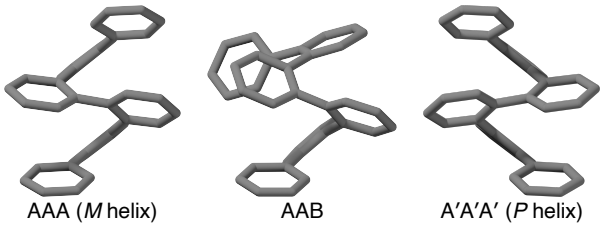

Figure 1: The AAA, AAB, and A′A′A′ conformers of (unsubstituted) hexa(*o*-phenylene).

2.2 Conformational analysis

We first briefly summarize the folding behavior of *o*-phenylenes.[27] The folding state of an *o*-phenylene [*n*]-mer is defined by the $n-3$ internal torsional angles ϕ_i along its backbone (ϕ_2–ϕ_4 in Figure 2). Each key dihedral can assume one of four values that we name using a simple system, where "A" represents $\phi_i \approx -55°$, "A′" $+55°$, "B" $+135°$, and "B′" $-135°$. Because every second ring must be nearly parallel, as has been previously discussed,[27] only ϕ_i differing by roughly 180° can coexist within a single molecule. Consequently, the total population of conformers can be divided into enantiomeric A/B and A′/B′ sets (i.e., the A/A′, B/B′, A/B′, etc., combinations are not possible within the same molecule). Examples of typical conformers for an *o*-phenylene hexamer are shown in Figure 1. When perfectly folded, all the biaryl torsional angles are in the A or A′ state ($\phi = -55°$ or $+55°$) corresponding to an *M* (left-handed) helix in the "AAA" state or a *P* (right-handed) helix in the "A′A′A′" state. In misfolded conformations, one or more torsional angles are in the B or B′ states. Misfolding of *o*-phenylenes tends to occur preferentially at the ends; thus, the "AAB" (or "A′A′B′") conformers should be the most populated misfolded states of a hexamer.

As expected, the NMR spectra of the new *o*-phenylene hexamers in $CDCl_3$ are complex, with contributions from multiple conformers. Broadened signals were observed close to room temperature because of intermediate rates of conformational exchange. This is typical of *o*-phenylenes; however, even at 278 K, the temperature usually used for our studies, the signals are still broad, implying that these oligomers undergo some conformational exchange process distinct from those of previously studied *o*-phenylenes. NMR spectra were therefore

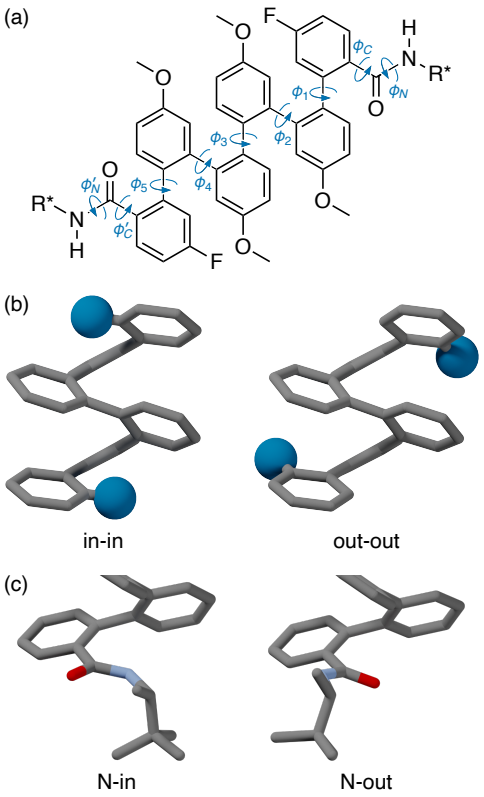

Figure 2: (a) Key dihedral angles determining distinguishable conformations of *o*-phenylene hexamer amides. (b) "In-in" and "out-out" orientations of terminal substituents differing in ϕ_1/ϕ_5. (c) "N-in" and "N-out" orientations of the amides differing in ϕ_C.

recorded at 266 K.

Many degrees of conformational freedom must be considered for these *o*-phenylene hexamers, corresponding to rotation about the bonds shown in Figure 2. First, there is the overall backbone configuration. This corresponds to interconversion between the enantiomeric A/B and A′/B′ populations described above, which requires simultaneous changes in all of ϕ_2–ϕ_4. This process has been studied in detail by Fukushima and Aida.[28,37] Second, there is backbone folding. Changes in individual dihedrals ϕ_2–ϕ_4 alter the folding state of the *o*-phenylene (e.g., perfectly folded AAA vs misfolded AAB). This process has been studied by us, and logically must be faster than backbone inversion.[27] Third, there is the cis vs trans configuration of the amides. Changes in ϕ_N are expected to be slow on the NMR time scale,[38–40] but the trans amide is expected to be substantially more stable than cis.[41,42] Thus ϕ_N is not likely to contribute meaningfully populated alternate conformers since the trans form should predominate. This is confirmed by DFT studies of model systems described in the Supporting Information. Fourth, there is the orientation of termini. Changes in ϕ_1 or ϕ_5 result in inequivalent conformers with the amide groups overall oriented inward, along the path of the helix, or outward, toward the side of the helix. There are therefore "in-in", "out-out", and "in-out" configurations likely to be present, shown in Figure 2b. The oligomer is still "well-folded" in all three cases since the repeat units still describe a helix. In general, these changes in terminus orientation (ϕ_1/ϕ_5) are expected to be slow by NMR spectroscopy so long as there are substituents ortho to the backbone connectivity (i.e., the amides).[35,37] The different conformers were distinguishable for our previously studied imines.[29]

Finally, there is the amide orientation, defined by ϕ_C, which deserves special comment. Rotation about this bond will place the nitrogen atom of the amide either inward-facing ("N-in") or outward-facing ("N-out"), as shown in Figure 2c. For a typical benzamide this process would be expected to be fast on the NMR time scale. However, if the whole amide is oriented inward, folding of the *o*-phenylene places it directly below the third ring along the backbone, which should hinder rotation. Calculated potential energy surfaces for model

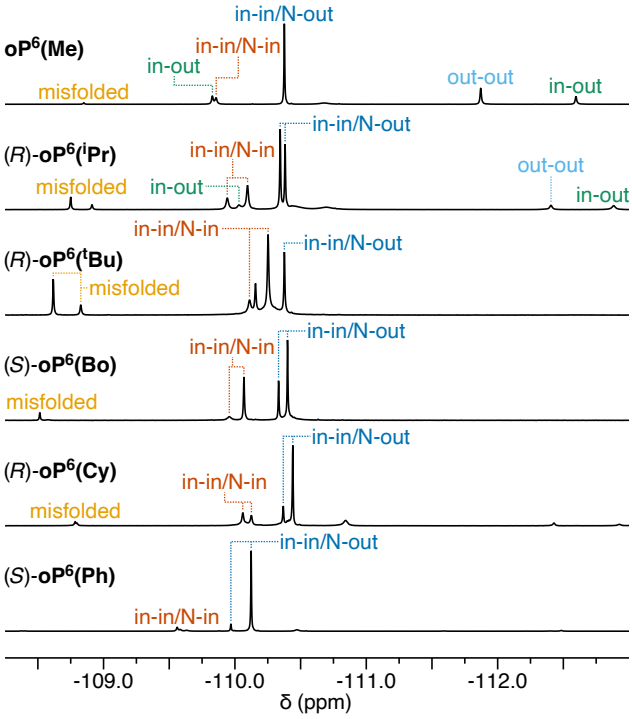

Figure 3: $^{19}F\{^1H\}$ NMR spectra of *o*-phenylene hexamers (376 MHz, $CDCl_3$, 266 K, 22–27 mM).

structures confirm this (see Supporting Information). Similar behavior might also be expected for the previously studied imines (i.e., Chart 1a), where it was not observed. DFT calculations show that the imines show a much stronger bias toward the N-out conformation compared to the amides and consequently this is likely the only meaningfully populated orientation (3.5 vs 0.4 kcal/mol at the PCM($CHCl_3$)/ωB97-XD/cc-pVDZ level), see Supporting Information). Thus, it seems very likely that amide reorientation via ϕ_C is the "new" conformational process that requires these systems to be analyzed at lower temperatures than other *o*-phenylenes. Note that we would only expect this to be an issue for inward-pointing amides in well-folded *o*-phenylenes, since otherwise the amide is not folded underneath the helix and its rotation would not be hindered.

The "achiral" (really dynamic racemate) **oP^6(Me)** provides a useful basis for understanding the behavior of the other hexamers. Its $^{19}F\{^1H\}$ NMR spectrum is shown in Figure 3 (top). The spectrum shows a large signal at −110.4 ppm corresponding to one predominant

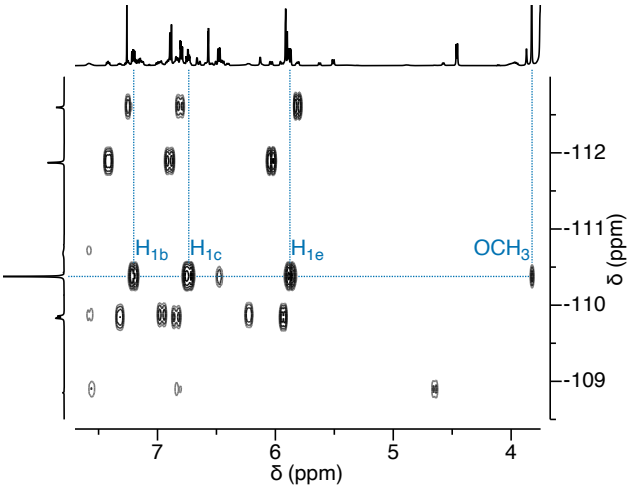

Figure 4: ^{19}F–^{1}H COSY NMR spectrum of **oP^{6}(Me)** (400 MHz, $CDCl_3$, 266 K). Correlations with H_{1b}, H_{1c}, and H_{1e}, and a methoxy group, for the major conformer are highlighted.

conformer with some other smaller signals related to minor conformers. We confirmed that these smaller signals are not due to impurities using ^{19}F–^{19}F EXSY spectroscopy, which shows clear cross-peaks with the major signal indicating chemical exchange. The complete proton assignments of the major conformer could be done using standard 2D NMR experiments (COSY, ^{19}F–^{1}H COSY, TOCSY, HMBC, and HSQC). Full chemical shift assignments were not possible for the minor conformers as their signals were weak and some key HMBC correlations were missing. Nevertheless, the ^{19}F–^{1}H COSY spectrum, shown in Figure 4, could be used to unambiguously assign at least the protons of the terminal rings (H_{1b}, H_{1c}, and H_{1e}, Chart 1) for every conformer detected in this system. These three protons are particularly useful for distinguishing different conformers as they undergo large changes in environment as the geometry changes. These assignments were further confirmed by ^{1}H–^{1}H EXSY (i.e., via cross peaks between different assigned H_{1b}, H_{1c}, and H_{1e}).

The single ^{19}F signal for the major conformer shows that it has twofold symmetry. The ^{1}H chemical shifts from rings 2 and 3 (Chart 1) indicate that it is well folded in the helical AAA/A′A′A′ states, as key protons (notably H_{2e} and H_{3e}) are very shielded (5.92 and 5.91 ppm), consistent with their positioning directly into the shielding zones of nearby aromatic rings (rings 5 and 6, respectively). Similar behavior has been observed in many other

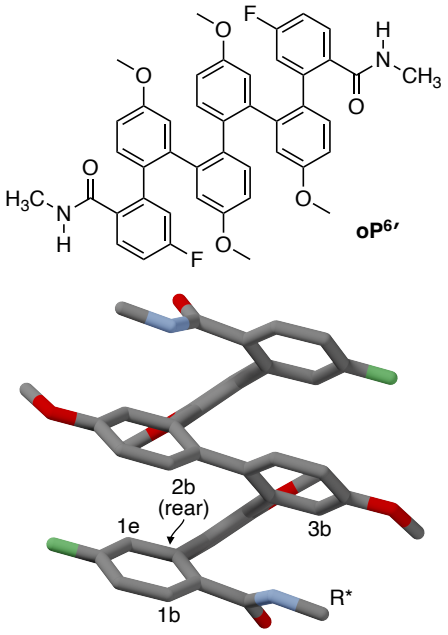

Figure 5: Model structure **oP$^{6\prime}$** and its in-in/N-out geometry optimized at the PCM($CHCl_3$)/ωB97-XD/cc-pVDZ level. Key positions referred to in the text are indicated.

o-phenylene systems.[27]

This most-intense signal in the ^{19}F NMR spectrum therefore corresponds to a well-folded *o*-phenylene, but what are the overall orientations of the termini (ϕ_1/ϕ_5) and amides (ϕ_C/ϕ'_C)? To better understand these different possible conformers, we optimized different geometries of model compound **oP$^{6\prime}$**, shown in Figure 5, at the PCM($CHCl_3$)/ωB97-XD/cc-pVDZ level. The optimized geometries of the in-in/N-out, in-in/N-in, and out-out conformers suggest spatial relationships that can be used to distinguish them spectroscopically.

The evidence indicates that the major conformer of **oP^6(Me)** has the in-in orientation of the termini and the N-out orientation of the amides, shown in Figure 5 for **oP$^{6\prime}$**. First, the signals for protons H_{1e} and the methine proton of the isopropyl group (R*) show ROE cross-peaks with the signals assigned to H_{2b} and H_{3b}, respectively; modeling indicates that the inward-facing terminus geometry puts these nuclei in close proximity. Second, the ^{19}F signal for the major conformer is deshielded compared to most others. Inward-facing amides at the termini put the fluoro groups out of the shielding zone of the stacked ring, and the

opposite is true for outward-facing termini. DFT-predicted ^{19}F isotropic shieldings support this assignment (Table S8). Third, there is a weak cross-peak in the ^{19}F–^{1}H COSY between the fluorine peak of the major conformer and one of the OCH_3 peaks. This indicates an outward-facing fluoro group (and thus inward-facing amide) that is close to one of the OCH_3 groups (e.g., F from ring 1 is close to OCH_3 on ring 3′), perhaps giving a weak F–H hydrogen bond. Similar behavior has been found to give coupling in other folded systems.[43] This issue is discussed further in the Supporting Information. Fourth, the signal for the N–H proton shows an ROE cross-peak with that of proton H_{1b}. This suggests that the amide group is oriented N-out to put these protons in close proximity (2.4 Å for N-out vs 4.3 Å for N-in in the model). Fifth, the N–H proton is more shielded for the major conformer than it is for the minor conformers (identified in the EXSY). The amide N-out conformer puts this proton into the center of the shielding zone of ring 3 (for the N–H on ring 1), whereas if it is N-in it is no longer well-aligned with this ring, consistent with DFT predictions of the shieldings (Table S8).

The minor signal at −109.9 ppm in the ^{19}F spectrum can then be assigned to the in-in/N-in conformer. Proton H_{1e} from this conformer shows an ROE cross-peak with H_{2b} showing that the termini are overall still inward-facing. The N-in orientation of the amide can be determined by the process of elimination, but is supported by the changes in chemical shifts for protons H_{1b}, H_{1c}, and H_{1e} and the fluorines. All are deshielded compared to their counterparts in the major (N-out) conformer. This is especially pronounced for proton H_{1b}, which would be in the deshielding zone of the carbonyl group for the N-in conformer but not N-out. The effect on the chemical shifts of H_{1c}, H_{1e}, and the fluorine is likely due to increased electron-withdrawing power of the amide group in the N-in conformer. DFT models predict it to be less-twisted with respect to the ring in this orientation and thus more-strongly conjugated (33° vs 45° for $\mathbf{oP^{6\prime}}$).

The ^{19}F signal in the more-shielded region (at −111.9 ppm) is assigned to the out-out conformer. The proton H_{1e} related to this conformer shows an ROE cross-peak with H_{3b},

consistent with the out-out geometry, which puts H_{1e} and H_{3b} in close proximity. In this case we cannot distinguish different amide orientations, which is reasonable as rotation about ϕ_C ought not to be hindered by the folded oligomeric backbone when the amide is facing outward (or because the population of one conformer is low and cannot be detected). The downfield ^{19}F signal at −108.9 ppm corresponds to the misfolded (AAB) geometry. This is very clear from the F–H COSY spectrum: this peak shows cross-peak with an aromatic proton (H_{1e}) at about 4.7 ppm (Figure 4). This extreme shielding is a signature of the AAB conformer found in other *o*-phenylene systems.[35] The corresponding signal for the other end of the AAB conformer is not obvious for **oP^6(Me)**, but from the other oligomers (see below) it appears to be broadened around −110 to −111 ppm. The two other signals with equal intensities (at −109.8 and −112.6 ppm) must be from the in-out conformers on the basis of their symmetry. The overall populations of the different conformers for **oP^6(Me)** were obtained by deconvolution of the ^{19}F{^{1}H} NMR spectrum and are given in Table 1.

The ^{19}F{^{1}H} NMR spectrum of (*R*)-**oP^6(i Pr)** (Figure 3) is similar to that of **oP^6(Me)** but with doubling of the major peaks, indicating distinguishable diastereomeric twist senses because of the chirality centers. The ^{19}F–^{1}H COSY spectrum was especially important for making assignments. The two cross-peaks for proton H_{1e} of the in-in/N-out conformer are <6.0 ppm, the same as **oP^6(Me)**. Similarly, the peak assigned to the in-in/N-in form gives cross-peaks closer to 6.2 ppm, and that for the misfolded one was observed around 4.6 ppm. Splitting of the main peaks suggests a low de of (16 ± 7)% for the in-in/N-out form while the in-in/N-in form and misfolded form appear to have higher (but still modest) de's of (30 ± 6)% and (36 ± 6)%, respectively. The proportion of outward-facing amides is smaller than in the achiral oligomer, but the proportions of minor misfolded and in-in/N-in conformers have increased for **oP^6(i Pr)**.

The ^{19}F{^{1}H} spectra of the other *o*-phenylene hexamers with different chiral amide groups are shown in Figure 3. Deconvolution of the ^{19}F{^{1}H} NMR spectra allowed us to extract the relative populations and diastereomeric excesses of different conformations present for

Compound	Overall twist sense	Conformer	Population (%)	de (%)
oP^6(Me)	n.a.	in-in/N-out	40 ± 5	n.a.
		in-in/N-in	10 ± 1	n.a.
		in-out	19 ± 2	n.a.
		out-out	18 ± 2	n.a.
		misfolded	2.9 ± 0.3	n.a.
(*R*)-**oP^6(iPr)**	*P*	in-in/N-out	41 ± 3	16 ± 7
		in-in/N-in	24 ± 2	30 ± 6
		in-out	10.2 ± 0.8	n.d.
		out-out	3.7 ± 0.4	n.d.
		misfolded	13.2 ± 1.1	36 ± 6
(*R*)-**oP^6(Cy)**	*P*	in-in/N-out	49 ± 4	60 ± 5
		in-in/N-in	21 ± 2	15 ± 7
		out-out	3.9 ± 0.4	n.d.
		misfolded	10.2 ± 0.8	38 ± 6
(*S*)-**oP^6(Ph)**	*M*	in-in/N-out	73 ± 8	82 ± 2
		in-in/N-in	10 ± 1	29 ± 6
		out-out	0.67 ± 0.08	n.d.
		misfolded	2.2 ± 0.2	6 ± 7
(*R*)-**oP^6(^{t}Bu)**	*P*	in-in/N-out	n.d.	>90
		in-in/N-in	n.d. (high)	53 ± 5
		misfolded	n.d. (high)	40 ± 6
(*S*)-**oP^6(Bo)**	*M*	in-in/N-out	53 ± 5	32 ± 6
		in-in/N-in	35 ± 3	54 ± 5
		misfolded	11 ± 1	63 ± 4

Table 1: Twist sense control in *o*-phenylene hexamers. Errors calculated assuming a 10% uncertainty on integration.

these compounds (see Table 1). For **oP^6(^{t}Bu)**, it is clear that the populations of both misfolded and in-in/N-in conformers have increased significantly; however, we were unable to definitively quantify the populations because of additional overlapping signals, likely because of the now-significantly populated misfolded conformers.

The helical twist sense of the chiral oligomers was further investigated by CD spectroscopy carried out in chloroform at room temperature. All of the chiral hexamers show significant CD bands, as shown in Figure 6. We were particularly interested in the compounds with the saturated chiral groups (**oP^6(^{t}Bu)**, **oP^6(^{i}Pr)**, **oP^6(Cy)**, **oP^6(Bo)**) because absorption ≥230 nm should be centered on the *o*-phenylene moiety and the resulting CD signals should

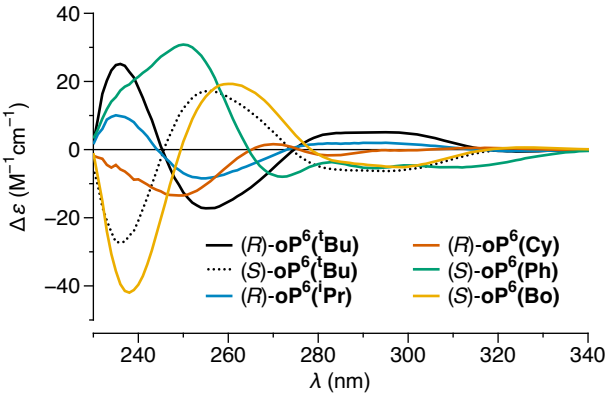

Figure 6: Experimental CD spectra of *o*-phenylene hexamers ($CHCl_3$).

thus reflect the twist sense of the *o*-phenylene backbone. The CD spectra of (*R*)- and (*S*)-**oP^6(^{t}Bu)**, (*R*)-**oP^6(^{i}Pr)**, and (*S*)-**oP^6(Bo)** have nearly identical shapes, with key Cotton effects at approximately 257 and 295 nm. (*R*)-**oP^6(Cy)** shows a slightly different CD spectrum with Cotton effects at approximately 250 and 270 nm. The CD spectrum of (*S*)-**oP^6(Ph)** has a shoulder at around 238 nm. This peak is because of the excitation of the chiral group itself (determined by comparison with the CD spectrum of *N*-(1-phenylethyl)benzamide, Figure S2), but the peak at 250 nm is assigned to the *o*-phenylene backbone.

To assign the absolute configurations of the *o*-phenylene backbones, we predicted CD spectra for model compound **oP$^{6\prime}$** using TD-DFT at the PCM($CHCl_3$)/CAM-B3LYP/6-311+G(2d,2p)//PCM($CHCl_3$)/wB97-XD/cc-pVDZ level. The predicted CD spectra match the shapes of the experimental CD spectra, particularly for **oP^6(^{i}Pr)**, **oP^6(Cy)**, **oP^6(^{t}Bu)**, and **oP^6(Bo)**. The Cotton effect around 250–260 nm can be used to determine the absolute twist sense in these systems. A positive Cotton effect around 250–260 nm is associated with the *M* twist sense of the helix. The overall absolute twist senses of these *o*-phenylene hexamers with different chiral amide groups were assigned on this basis and are compiled in Table 1.

3 Discussion

The CD and NMR spectroscopy experiments were carried out a different temperatures, and so the conformational distributions should not be identical. However, some conclusions can be drawn about chiral induction and conformational effects for this series of compounds using the data in Table 1. First, the amide-functionalized *o*-phenylenes have a stronger preference for inward-facing termini compared to the previous imine-functionalized *o*-phenylenes (Chart 1a), which gave mixtures of both in-in and out-out conformers.[29] This may suggest that amide groups interact more strongly with the third benzene ring up the oligomer. Second, the populations of the out-out conformers in the amide series decrease with an increase in the bulkiness of the chiral group, such that it is not detected for **oP^6(^{t}Bu)** and **oP^6(Bo)**. In the outward-facing conformers, the amide group is placed closer to the helix and increasing the bulkiness of chiral groups appears to result in additional steric clashes with the *o*-phenylene backbone. This result is consistent with previous work that has shown a preference for inward-facing substituents at *o*-phenylene termini.[37] Third, the bulkiness of chiral groups generally increases misfolding and the proportion of N-in conformers, likely simply because of steric effects (e.g., in the misfolded AAB conformer, the substituent is necessarily farther from the *o*-phenylene helix). Fourth, **oP^6(Ph)** shows both the highest proportion of the in-in/N-out conformer and the highest de for this conformer. The reason for this is not immediately obvious, although it does suggest that there may be some repulsive interaction between the phenyl group and the *o*-phenylene exterior that contributes to efficient chiral induction.

While the overall conformational picture in Table 1 is complicated, we note that for the structurally simpler **oP^6(^{i}Pr)**, **oP^6(^{t}Bu)**, **oP^6(Cy)**, and **oP^6(Ph)**, for which the absolute configuration corresponds to the simple arrangement of groups of different steric demand, the *R* configuration of the chirality center consistently gives the *P* configuration of the helix (and *S* gives *M*) in the (usually dominant) in-in/N-out conformer. This is the case for **oP^6(Ph)**, which is the best performing of the oligomers in the sense of most-efficient chiral induction.

The trend matches the results of the previously reported imines and lends itself to a simple model, shown in Figure 7a, that is possible because of the detailed conformational analysis of these *o*-phenylenes. There is a strong preference for the proton attached to the chirality centers (the small group) to be antiperiplanar to the amide hydrogen. This behavior is consistent with that of amides used to establish the absolute configurations of chiral amines by NMR spectroscopy[44] and is confirmed in the present systems by DFT calculations (see Supporting Information). This constraint is sufficient to orient the chirality center with respect to the helix in the in-in/N-out state. The *R* configuration of the chirality center is then favorable for the *P* configuration of the helix because it orients the large group away from the *o*-phenylene. With the *M* helix a steric clash between the large group and the helix is unavoidable. Application of this model to a simple analogue of (*R*)-**oP^6(Ph)** using DFT calculations is shown in Figure 7b. While the *P* helix is a good match to the configuration of the chirality center, the *M* helix is directed toward the phenyl group, introducing small, but meaningful, strain.

In biochemistry, the inspiration for the foldamers field, small chemical changes can drive large amplitude changes in geometry.[32] Understanding the fine details of how substituents interact with folded backbones is key to achieving similar behavior in abiotic systems. The results here show that a reasonably small change in functional group structure, imine to amide, can have a substantial effect on folding, affecting broad conformational behavior (e.g., prevalence inward- vs outward-facing termini via ϕ_1/ϕ_5) and introducing new variability (amide orientation via ϕ_C). These changes can nevertheless be understood using simple models for folding in polyphenylene systems. The next logical step is to explore how different substituents attached to the same backbone interact through these conformational effects.

The results also highlight the detailed information on conformational behavior that can be obtained for sterically congested polyphenylenes by NMR spectroscopy, and in particular the usefulness of ^{19}F labeling.

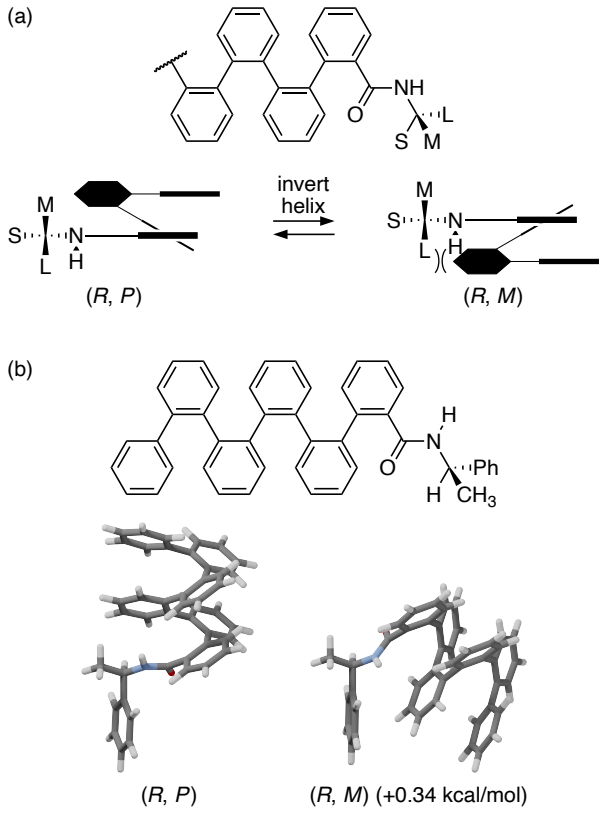

Figure 7: (a) Model describing chiral induction for inward-oriented, N-out *o*-phenylene amides (S = small, M = medium, L = large). (b) Optimized geometries of a simple analogue of (*R*)-**oP^6(Ph)** according to the model (PCM($CHCl_3$)/ωB97X-D/cc-pVDZ).

3.1 Conclusion

In summary, we have investigated the conformational behavior of *o*-phenylenes with amide groups attached at their termini. A detailed picture of conformer distributions has been obtained by a combination of NMR spectroscopy, CD spectroscopy, and computational methods. For the *o*-phenylene amides studied here, the termini prefer to be oriented inward. Conformers differing in the orientation of the amide can be distinguished, with the N-out orientation favored, particularly for amides that are less sterically demanding. The configurations of the terminal amide groups has been effectively transmitted to the *o*-phenylene backbone, leading to the preferential one-handed helicity. Chiral induction is particularly effective from the phenyl-substituted amide **oP^6(Ph)** and can be predicted using a simple model based on sterics.

Acknowledgements

We thank the National Science Foundation for support of this work (CHE-1904236) and the purchase of the 400 MHz NMR spectrometer (CHE-1919850).

Supporting Information

NMR assignments, computational chemistry details, experimental procedures, NMR spectra of synthesized compounds (PDF)

Cartesian coordinates for optimized geometries (TXT)

The data underlying this study are openly available in the *Miami Scholarly Commons* at http://hdl.handle.net/2374.MIA/6834.

References

(1) Gellman, S. H. Foldamers: a manifesto. *Acc. Chem. Res.* **1998**, *31*, 173–180.

(2) Hill, D. J.; Mio, M. J.; Prince, R. B.; Hughes, T. S.; Moore, J. S. A field guide to foldamers. *Chem. Rev.* **2001**, *101*, 3893–4011.

(3) Guichard, G.; Huc, I. Synthetic foldamers. *Chem. Commun.* **2011**, *47*, 5933–5941.

(4) Zhang, D.-W.; Zhao, X.; Hou, J.-L.; Li, Z.-T. Aromatic amide foldamers: structures, properties, and functions. *Chem. Rev.* **2012**, *112*, 5271–5316.

(5) Ferrand, Y.; Huc, I. Designing helical molecular capsules based on folded aromatic amide oligomers. *Acc. Chem. Res.* **2018**, *51*, 970–977.

(6) Ikkanda, B. A.; Iverson, B. L. Exploiting the interactions of aromatic units for folding and assembly in aqueous environments. *Chem. Commun.* **2016**, *52*, 7752–7759.

(7) Legrand, B.; Aguesseau-Kondrotas, J.; Simon, M.; Maillard, L. Catalytic foldamers: When the structure guides the function. *Catalysts* **2020**, *10*, 700.

(8) Chandramouli, N.; Ferrand, Y.; Lautrette, G.; Kauffmann, B.; Mackereth, C. D.; Laguerre, M.; Dubreuil, D.; Huc, I. Iterative design of a helically folded aromatic oligoamide sequence for the selective encapsulation of fructose. *Nat. Chem.* **2015**, *7*, 334–341.

(9) Kim, M. J.; Choi, Y. R.; Jeon, H.-G.; Kang, P.; Choi, M.-G.; Jeong, K.-S. A helically twisted imine macrocycle that allows for determining the absolute configuration of α-amino carboxylates. *Chem. Commun.* **2013**, *49*, 11412–11414.

(10) Tanatani, A.; Yokoyama, A.; Azumaya, I.; Takakura, Y.; Mitsui, C.; Shiro, M.; Uchiyama, M.; Muranaka, A.; Kobayashi, N.; Yokozawa, T. Helical structures of *N*-alkylated poly(*p*-benzamide)s. *J. Am. Chem. Soc.* **2005**, *127*, 8553–8561.

(11) Kudo, M.; Hanashima, T.; Muranaka, A.; Sato, H.; Uchiyama, M.; Azumaya, I.; Hirano, T.; Kagechika, H.; Tanatani, A. Identification of absolute helical structures of aromatic multilayered oligo(*m*-phenylurea)s in solution. *J. Org. Chem.* **2009**, *74*, 8154–8163.

(12) Jang, H. B.; Choi, Y. R.; Jeong, K.-S. Matched and mismatched phenomena in the helix orientation bias induced by chiral appendages at multiple positions of indolocarbazole-pyridine hybrid foldamers. *J. Org. Chem.* **2018**, *83*, 5123–5131.

(13) Jiang, J.; Slutsky, M. M.; Jones, T. V.; Tew, G. N. Apolar *ortho*-phenylene ethynylene oligomers: conformational ordering without intermolecular aggregation. *New J. Chem.* **2010**, *34*, 307–312.

(14) Prince, R. B.; Brunsveld, L.; Meijer, E. W.; Moore, J. S. Twist sense bias induced by chiral side chains in helically folded oligomers. *Angew. Chem., Int. Ed.* **2000**, *39*, 228–230.

(15) Mazzier, D.; Crisma, M.; De Poli, M.; Marafon, G.; Peggion, C.; Clayden, J.; Moretto, A. Helical foldamers incorporating photoswitchable residues for light-mediated modulation of conformational preference. *J. Am. Chem. Soc.* **2016**, *138*, 8007–8018.

(16) Le Bailly, B. A. F.; Clayden, J. Dynamic foldamer chemistry. *Chem. Commun.* **2016**, *52*, 4852–4863.

(17) Kim, J.; Jeon, H.-G.; Kang, P.; Jeong, K.-S. Stereospecific control of the helical orientation of indolocarbazole–pyridine hybrid foldamers by rational modification of terminal chiral appendages. *Chem. Commun.* **2017**, *53*, 6508–6511.

(18) Liu, Z.; Hu, X.; Abramyan, A. M.; Mészáros, Á.; Csékei, M.; Kotschy, A.; Huc, I.; Pophristic, V. Computational prediction and rationalization, and experimental validation of handedness induction in helical aromatic oligoamide foldamers. *Chem.—Eur. J.* **2017**, *23*, 3605–3615.

(19) Zheng, L.; Zhan, Y.; Yu, C.; Huang, F.; Wang, Y.; Jiang, H. Controlling helix sense at N- and C-termini in quinoline oligoamide foldamers by β-pinene-derived pyridyl moieties. *Org. Lett.* **2017**, *19*, 1482–1485.

(20) Clayden, J.; Castellanos, A.; Solà, J.; Morris, G. A. Quantifying end-to-end conformational communication of chirality through an achiral peptide chain. *Angew. Chem., Int. Ed.* **2009**, *48*, 5962–5965.

(21) Dong, Z.; Plampin III, J. N.; Yap, G. P. A.; Fox, J. M. Minimalist end groups for control of absolute helicity in salen- and salophen-based metallofoldamers. *Org. Lett.* **2010**, *12*, 4002–4005.

(22) Dolain, C; Jiang, H; Léger, J.; Guionneau, P; Huc, I. Chiral induction in quinoline-derived oligoamide foldamers: assignment of helical handedness and role of steric effects. *J. Am. Chem. Soc.* **2005**, *127*, 12943–12951.

(23) Dong, Z.; Karpowicz Jr., R. J.; Bai, S.; Yap, G. P. A.; Fox, J. M. Control of absolute helicity in single-stranded abiotic metallofoldamers. *J. Am. Chem. Soc.* **2006**, *128*, 14242–14243.

(24) Kendhale, A. M.; Poniman, L.; Dong, Z.; Laxmi-Reddy, K.; Kauffmann, B.; Ferrand, Y.; Huc, I. Absolute control of helical handedness in quinoline oligoamides. *J. Org. Chem.* **2010**, *76*, 195–200.

(25) Hu, H.-Y.; Xiang, J.-F.; Yang, Y.; Chen, C.-F. Chiral induction in phenanthroline-derived oligoamide foldamers: an acid- and base-controllable switch in helical molecular strands. *Org. Lett.* **2008**, *10*, 1275–1278.

(26) Naidu, V. R.; Kim, M. C.; Suk, J.-m.; Kim, H.-J.; Lee, M.; Sim, E.; Jeong, K.-S. Biased helical folding of chiral oligoindole foldamers. *Org. Lett.* **2008**, *10*, 5373–5376.

(27) Hartley, C. S. Folding of *ortho*-phenylenes. *Acc. Chem. Res.* **2016**, *49*, 646–654.

(28) Ohta, E.; Sato, H.; Ando, S.; Kosaka, A.; Fukushima, T.; Hashizume, D.; Yamasaki, M.; Hasegawa, K.; Muraoka, A.; Ushiyama, H.; Yamashita, K.; Aida, T. Redox-responsive molecular helices with highly condensed π-clouds. *Nat. Chem.* **2011**, *3*, 68–73.

(29) Vemuri, G. N.; Pandian, R. R.; Spinello, B. J.; Stopler, E. B.; Kinney, Z. J.; Hartley, C. S. Twist sense control in terminally functionalized *ortho*-phenylenes. *Chem. Sci.* **2018**, *9*, 8260–8270.

(30) Brown, R. A.; Diemer, V.; Webb, S. J.; Clayden, J. End-to-end conformational communication through a synthetic purinergic receptor by ligand-induced helicity switching. *Nat. Chem.* **2013**, *5*, 853–860.

(31) Solà, J.; Fletcher, S. P.; Castellanos, A.; Clayden, J. Nanometer-range communication of stereochemical information by reversible switching of molecular helicity. *Angew. Chem., Int. Ed.* **2010**, *49*, 6836–6839.

(32) Boehr, D. D.; Nussinov, R.; Wright, P. E. The role of dynamic conformational ensembles in biomolecular recognition. *Nat. Chem. Biol.* **2009**, *5*, 789–796.

(33) Rowan, S. J.; Cantrill, S. J.; Cousins, G. R. L.; Sanders, J. K. M.; Stoddart, J. F. Dynamic covalent chemistry. *Angew. Chem., Int. Ed.* **2002**, *41*, 898–952.

(34) An initial version of this work was deposited in *ChemRxiv* on Jul. 22, 2022, Reference DOI: 10.26434/chemrxiv-2022-r1hd3.

(35) Mathew, S.; Crandall, L. A.; Ziegler, C. J.; Hartley, C. S. Enhanced helical folding of *ortho*-phenylenes through the control of aromatic stacking interactions. *J. Am. Chem. Soc.* **2014**, *136*, 16666–16675.

(36) Kirinda, V. C.; Vemuri, G. N.; Kress, N. G.; Flynn, K. M.; Kumarage, N. D.; Schrage, B. R.; Tierney, D. L.; Ziegler, C. J.; Hartley, C. S. Fluorine labeling of *ortho*-phenylenes to facilitate conformational analysis. *J. Org. Chem.* **2021**, *86*, 15085–15095.

(37) Ando, S.; Ohta, E.; Kosaka, A.; Hashizume, D.; Koshino, H.; Fukushima, T.; Aida, T. Remarkable effects of terminal groups and solvents on helical folding of *o*-phenylene oligomers. *J. Am. Chem. Soc.* **2012**, *134*, 11084–11087.

(38) Sui, Q.; Borchardt, D.; Rabenstein, D. L. Kinetics and equilibria of cis/trans isomerization of backbone amide bonds in peptoids. *J. Am. Chem. Soc.* **2007**, *129*, 12042–12048.

(39) LaPlanche, L. A.; Rogers, M. T. Configurations in unsymmetrically N,N-disubstituted amides. *J. Am. Chem. Soc.* **1963**, *85*, 3728–3730.

(40) Akhdar, A.; Gautier, A.; Hjelmgaard, T.; Faure, S. *N*-Alkylated aromatic poly- and oligoamides. *ChemPlusChem* **2021**, *86*, 298–312.

(41) LaPlanche, L. A.; Rogers, M. T. *cis* and *trans* configurations of the peptide bond in N-monosubstituted amides by nuclear magnetic resonance. *J. Am. Chem. Soc.* **1964**, *86*, 337–341.

(42) Hallam, H.; Jones, C. M. Conformational isomerism of the amide group—A review of the IR and NMR spectroscopic evidence. *J. Mol. Struct.* **1970**, *5*, 1–19.

(43) Zornik, D.; Meudtner, R. M.; El Malah, T.; Thiele, C. M.; Hecht, S. Designing structural motifs for clickamers: Exploiting the 1,2,3-triazole moiety to generate conformationally restricted molecular architectures. *Chem.—Eur. J.* **2011**, *17*, 1473–1484.

(44) Trost, B. M.; Bunt, R. C.; Pulley, S. R. On the use of *O*-methylmandelic acid for the establishment of absolute configuration of α-chiral primary amines. *J. Org. Chem.* **1994**, *59*, 4202–4205.